

# Site-Specific Stochastic Spatio-Temporal Channel Model for Sub-Urban Slightly Non-Line-of-Sight Microcellular Environment

Jun-ichi TAKADA, Wataru HACHITANI, Ji-Ye FU and Houtao ZHU

Department of International Development Engineering,  
Tokyo Institute of Technology, Tokyo, 152-8552, Japan.  
takada@ide.titech.ac.jp

**Abstract** This paper reports a site-specific spatio-temporal channel model for the suburban slightly NLOS (non-line-of-sight) microcellular environment, based on the field test result of the azimuth-delay spectrum. The parameter extraction scheme of the spatio-temporal channel is briefly reviewed [1, 2], first. Then, the implementation issue of the stochastic spatio-temporal fading simulator is described. Finally, the fading parameters generated by the simulator are compared with the original data.

## Introduction

The introduction of microcell is necessary for the future wireless communication systems due to the following reasons:

**$E_b/N_0$  requirement:** The required  $E_b/N_0$ , signal energy per bit to noise power ratio, is independent of the transmission bit rate to obtain the same bit error rate (BER). Since  $N_0$  is the receiver RF front end noise, the transmission power must be proportional to the bit rate to realize the same  $E_b$ .

**Frequency characteristics of propagation loss:** In addition to the increase of the free space attenuation, the shadowing loss due to the buildings and the trees is increasing, in accordance with the increase of the frequency.

The authors have been involving in the spatio-temporal channel characterization of microcellular environments by raytracing simulation and experiments. In the previous study, the statistical model parameters of the spatio-temporal channel in the suburban slightly NLOS (non-line-of-sight) environment are extracted from the azimuth-delay spectrum [1, 2]. In this paper, the implementation issue of the stochastic spatio-temporal fading simulator based on these model parameters is described. The properties of the fading channel generated by the simulator are compared with the original data.

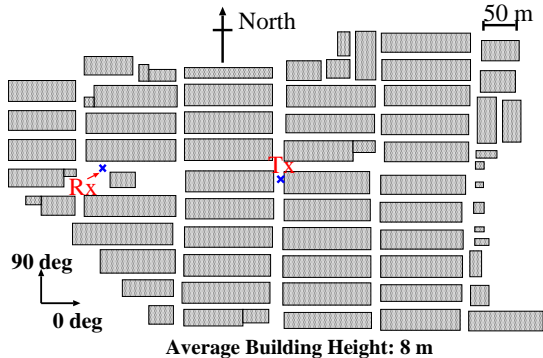


Figure 1: Yokosuka Highland Microcellular Environment.

### The Environment under Consideration

Figure 1 shows the map of Yokosuka Highland area, Kanagawa, Japan, the environment under consideration. It is a residential area with the wooden houses of 8 m high in average, and is considered as a typical suburban microcellular environment sized  $600 \times 600 \text{ m}^2$ . The traffic was very light, and the environment is considered to be static through the experiments. In this paper, the slightly NLOS transmitter and receiver shown in Fig. 1 are considered. As a transmitter antenna simulating the mobile station, vertically polarized omnidirectional half wave sleeve dipole was set at the height of 2.7 m. At the receiving point corresponding to the base station, the azimuth-delay spectrum was taken. It was measured by rotating the vertically polarized parabolic antenna with the beamwidth of about 4 deg. at the azimuth step of 4 deg. which was set at the height of 4.4 m. At each azimuth step, the delay spectrum was measured by using the delay profile measurement system [5]. At the center frequency of 8.45 GHz and with the chip rate of 50 Mcps, 7 stages M sequence with the dynamic range of 42 dB was transmitted, and the correlation receiver output the delay spectrum.

### Extraction of Spatio-Temporal Channel Parameters

The extraction scheme of spatio-temporal channel parameters is described in detail in Refs. [1, 2], and is briefly reviewed in this section.

The procedure to extract the model parameters is summarized as a flow chart in Fig. 2. The azimuth-delay spectrum is taken as the original data. The azimuth spectrum is first calculated to extract the forward arrival waves. Next, the delay spectrum for the forward arrival waves is approximated as the exponential function, and its fluctuation component is approximated as the stationary log-normal distribution. At the same time, the short term angular spread is approximated as the stationary normal distribution. Within the time resolution of the experimental setup, these two values are white in the delay domain, i.e. US (uncorrelated scattering) assumption is valid. The fluctuation component of the delay spectrum and the short term azimuth profile are negatively correlated. The Nakagami-Rice fading model is proposed for the short term azimuth spectrum to model this cross-correlation, as shown in Fig. 3. In this model, the average power is assumed to be exponentially decreasing, and the fluctuation component is modeled as the Rayleigh model with the constant angular spread. The stable signal is modeled as the log-normal distributed stationary process, with respect to the delay time. Contrary, the power of scattering components is deterministically modeled according to the exponential decay with respect to the delay time. The average Rician (or  $K$ ) factor and the angular spread of the Rayleigh component are jointly determined so as to satisfy the average and the standard

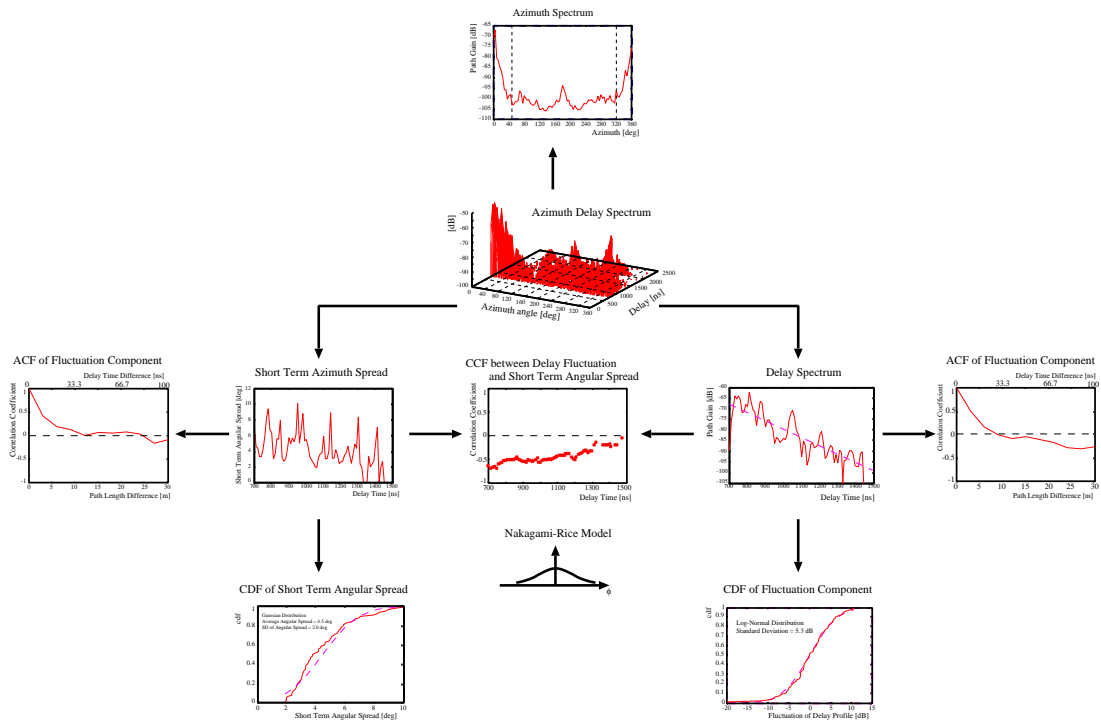


Figure 2: Flow Chart of Model Parameters Extraction Procedure from Azimuth-Delay Profile.

deviation of the angular spread. Under these assumption, the power increases and the azimuth spread decreases when the stable signal is large, i.e., they are negatively correlated.

It is noted that the parameters extracted from the experimental azimuth-delay spectrum is site-specific, i.e. they may vary in site-by-site, although the dominant mechanism described here may not drastically change.

### Stochastic Modeling of Spatio-Temporal Channel

Although the model parameters extracted in the manner as presented in the previous section, the stochastic modeling of the channel is necessary to evaluate the average transmission properties around the measurement points.

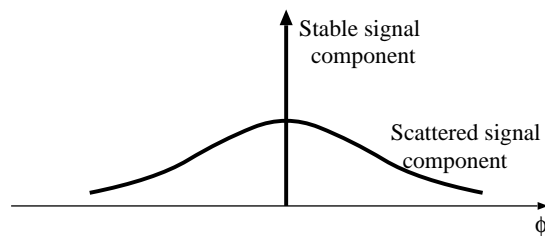


Figure 3: Nakagami-Rice Fading Model for Short Term Azimuth Profile.

### Model Structure

In the azimuth domain, discrete impulse model is used, i.e. each elementary wave is modeled as an impulse, and its azimuth value is not discretized. In the delay domain, contrary, the transversal filter model is used, i.e. the delay time is discretized with specific tap interval and each tap has its angular response. The snapshot model is described so far, but it can be used as the initial value of the dynamic model by taking into account the Doppler shift due to the motion of the mobile terminal and the angle of arrival of each path.

### Modeling Steps

At each delay tap, execute the following:

1. Generate the stable strong component.
  - Its average strength  $\bar{P}^s(\tau)$  is decided by exponentially decaying delay profile. and its standard deviation  $\Delta P^s$  is set to be constant. A real random number  $|P^s(\tau)|$  according to the log-normal distribution with the average and the SD (standard deviation) above is generated.
  - Its phase is according to the uniform distribution within  $[0, 2\pi)$ . A real random number  $\arg[P^s(\tau)]$  according to the uniform distribution above is generated.
  - Its azimuth angle  $\varphi^s(\tau)$  is set to be zero.
2. Generate the multipath component.
  - The angular spread of the Rayleigh component  $\Delta\varphi^m$ , the average Rician factor  $\bar{K}$ , and the total power of the multipath component  $P^m(\tau)$  are jointly determined so as to fit the skirt of the azimuth profile, the average and the standard deviation of the total angular spread, and the cross-correlation between the fluctuation component of the delay spectrum and the short term azimuth spread. The Gaussian distribution is assumed to model the angular profile of multipath component.
    - $L$  paths are assumed to compose the multipath, each path is assigned the power of  $P^m(\tau)/L$ .
    - Azimuth angle of each path is according to the Gaussian distribution with zero mean and the standard deviation equal to the angular spread. A real random number  $\varphi_l^m(\tau)$  is generated according to this distribution for  $l$ -th path.
    - The phase of each is according to the uniform distribution within  $[0, 2\pi)$ . A real random number  $\varphi_l^m(\tau)$  is generated according to this distribution for  $l$ -th path.

### Simulation Results

Based on the scheme presented in the previous section, the authors have implemented the spatio-temporal fading simulator. The results are compared with the experiments [1, 2].

Table 1 shows the specification of the simulation. It is noted that the azimuth spread and the average Rician factor are not optimized yet.

Figure 4 shows the delay spectra, which are in good coincidence, although faster fluctuation is observed for the simulation. The CDF (cumulative distribution function) of the fluctuation component of the delay spectrum from its exponential fit is shown in Fig. 5. They are completely in agreement, as is expected due to the modeling. The autocorrelation of this fluctuation component is presented in Fig. 6. Since the time resolution is 10 ns in the simulation and US assumption is applied, the correlation distance is smaller than the experiments.

Table 1: Specification of Simulation.

Decay of exponential delay spectrum	-0.038 dB/ns
Resolution of delay time $\Delta\tau$	10 ns
SD of fluctuation component of delay spectrum $\Delta P^s$	5.3 dB
Short term azimuth spread of scattering component $\Delta\varphi^m$	4.5 deg.
Average Rician factor $\bar{K}$	0 dB
Number of paths of scattering component per delay tap $L$	10

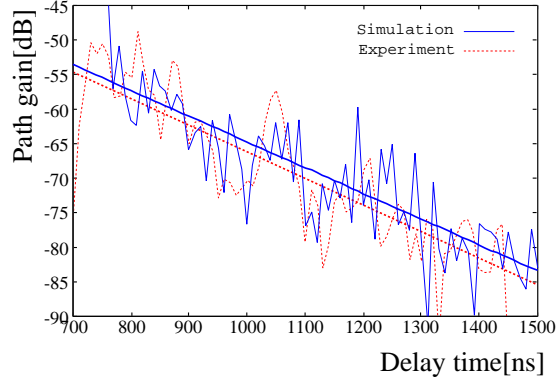


Figure 4: Delay Spectra.

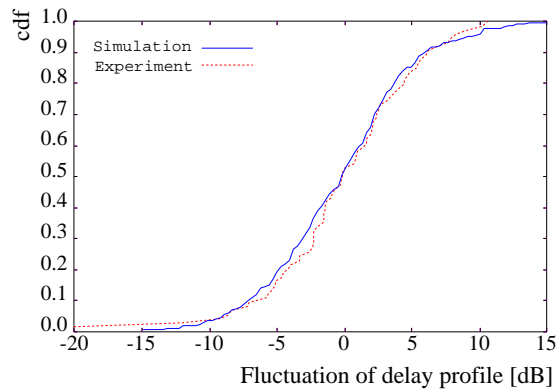


Figure 5: CDF of the Fluctuation Component of the Delay Profile from Its Exponential Fit.

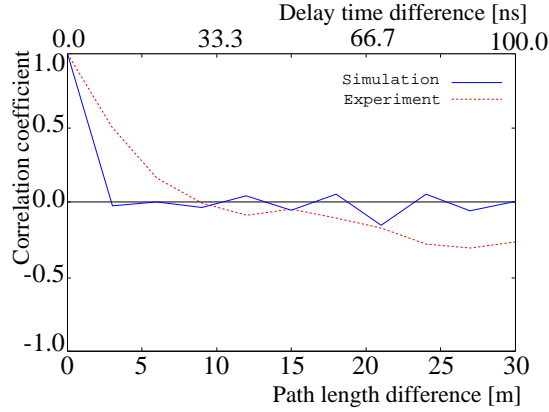


Figure 6: Autocorrelation of the Fluctuation Component of the Experimental Delay Profile from Its Exponential Fit.

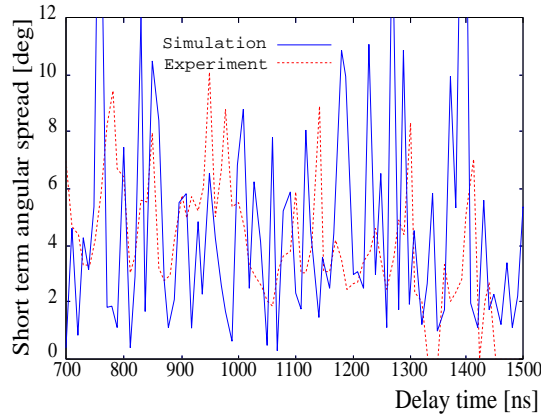


Figure 7: Short Term Azimuth Spread.

Figure 7 shows the short term angular spread, and Fig. 8 shows its CDF. As the azimuth spread of the scattering component and the Rician factor are not optimized, the deviation of the simulation result is bigger than the experiment. Figure 9 shows the autocorrelation function of the short-term azimuth spread. The result is very similar to Fig. 6 due to the US assumption in the modeling.

Unfortunately, the negative cross-correlation between the fluctuation component of the delay spectrum from its exponential fit and the short term azimuth spectrum has not been observed. Although the Nakagami-Rice model has been introduced, the Rician factor is assumed to be 0 dB, i.e. the model is almost Rayleigh. As far as Rayleigh model is concerned, the cross-correlation is expected to be zero.

## Conclusion and Future Works

This paper proposed the site-specific stochastic spatio-temporal channel modeling for the slightly NLOS suburban microcellular environment. The simulation results agreed well with the experimental results to some extent. The principal reason of the discrepancies is the inappropriate choice of the three parameters, i.e., the angular spread of the Rayleigh component  $\Delta\varphi^m$ , the average Rician factor  $\bar{K}$ , and the total power of the multipath component  $P^m(\tau)$ .

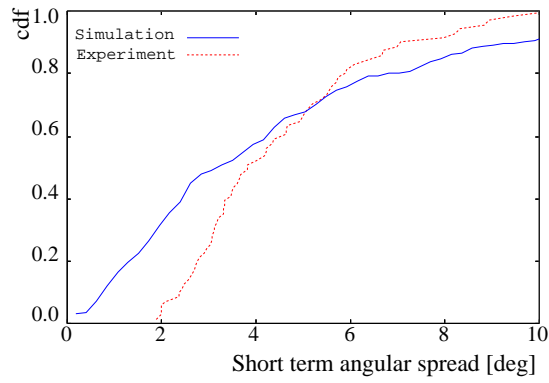


Figure 8: CDF of the Short-Term Azimuth Spread.

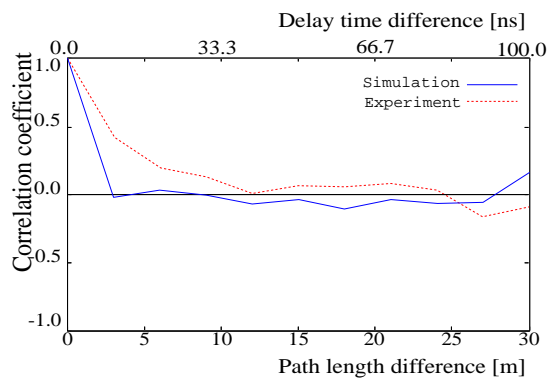


Figure 9: Autocorrelation of the Short Term Azimuth spread.

These three parameters are mutually related in the complicated manner. The following relations may be used for the improvement:

$$\Delta\varphi(\tau) = \frac{P^m \Delta\varphi^m}{P(\tau)}, \quad (1)$$

where  $P(\tau) = P^m + P^s(\tau)$  is the fluctuation component of the delay spectrum, and  $\Delta\varphi(\tau)$  is the short term azimuth spread. By averaging over the experimental delay spectrum, the product  $P^m \Delta\varphi^m$  is obtained as

$$P^m \Delta\varphi^m = \langle P(\tau) \Delta\varphi(\tau) \rangle. \quad (2)$$

On the other hand, the average Rician factor  $\bar{K}$  is determined so as to satisfy the cross-correlation property.  $P^m$  and  $\Delta\varphi^m$  are not separated in the formulation above, but  $\Delta\varphi^m$  shall be determined to fit the skirt of the average azimuth profile. The improved model considering these relations will be presented in the workshop.

This model is easily extended to MIMO model, since the Tx and Rx are set in the similar situations in the experiments, although it is left for future study.

### Acknowledgement

The authors are would like to thank Dr. T. Kobayashi, Mr. H. Shimizu, Mr. H. Masui, Mr. M. Ishii and Mr. K. Sakawa of YRP Key Tech Labs for their cooperation in the field tests. A part of the work was supported by the Scientific Research Grant-in-Aid from Japan Society for Promotion of Science.

### References

- [1] J. Takada, J. Fu, H. Zhu, T. Kobayashi: A Site-Specific Stochastic Spatio-Temporal Channel Modeling for Sub-Urban Non-Line-of-Sight Microcellular Environment. Proc. 4th Int. Symp. on Wireless Personal Multimedia Commun. (WPMC '01), pp. 767-772, Aalborg, Denmark, Sept. 2001.
- [2] J. Takada, J. Fu, H. Zhu, T. Kobayashi: Spatio-Temporal Channel Characterization in a Sub-Urban Non Line-of-Sight Microcellular Environment. IEEE J. Selected Areas in Commun., to be published.
- [3] H. Zhu, J. Takada, K. Araki, T. Kobayashi: Verification of a Two-Dimensional/Three-Dimensional Hybrid Ray-Tracing Method for Spatiotemporal Channel Modeling. Radio Science, vol. 36, no. 1, pp. 53-66, Jan.-Feb. 2001.
- [4] H. Zhu, J. Takada, K. Araki, T. Kobayashi: A Ray-Tracing-Based Characterization and Verification of the Spatio-Temporal Channel Model for Future Wideband Wireless Systems. IEICE Trans. Commun., vol. E84-B, no. 3, pp. 644-652, Mar. 2001.
- [5] H. Masui, K. Takahashi, S. Takahashi, K. Kage and T. Kobayashi, "Delay Profile Measurement System for Microwave Broadband Transmission and Analysis of Delay Characteristics in an Urban Environment," IEICE Trans. Electron., vol. E82-C, no. 7 pp. 1287-1292, July 1999.